Deslipping of Ester Rotaxanes: A Cooperative Interplay of Hydrogen Bonding with Rotational Barriers

Petra Linnartz,[a] Stephan Bitter,[a] and Christoph A. Schalley*[a]

Keywords: Supramolecular chemistry / Rotaxanes / Deslipping kinetics / Steric effects / Molecular devices

A series of rotaxanes has been synthesized which contain two ester groups in their axles. All rotaxanes bear the same tetralactam wheel. The kinetics of the de-slipping reaction of these rotaxanes were monitored in tetrachloroethane (TCE) and dimethyl sulfoxide (DMSO) resulting in the observation of a significant solvent effect. In TCE, two isomeric rotaxanes that differ merely with respect to the orientation of the ester groups show a remarkable difference in their deslipping behavior. When the ester carbonyl group is directly attached to the axle center piece, the rotaxane decomposes with a half life of ca. 10 h at 100 °C. The reverse orientation with the carbonyl group attached to the stopper blocks deslipping almost completely and a lower limit for the half life at 100 °C of 25,000 h was obtained. These results can be interpreted by inferring a cooperative action of hydrogen bonding between wheel and axle and differences in rotational barriers. Molecular modeling and AM1 calculations support this interpretation. The implications of these results for the determination of steric size and the optimization of molecular machines are discussed.

Introduction

The concept of steric size has been most useful for organic chemistry in that it helps to give a straightforward and intuitive explanation for the observed changes of reactivity with structure. Many attempts have been made in the past to accurately describe and determine the steric size of functional groups and substituents.[1] Some of them use the van der Waals surface of a molecule or substituent and describe the geometrical nature of steric size,[2] some definitions refer to reactivity and define steric effects as the enthalpic contributions of a certain change in a molecule to the change in reactivity, i.e. the reaction barrier.[3] Several scales of steric sizes have been defined including the most prominent A values, which are defined as the logarithm of the equilibrium constant of axial and equatorial substituents in the cyclohexane system.[4]

Quite recently, supramolecular chemistry offered a new way to approach the question of steric demand. It was suggested that the deslipping reaction[5] of rotaxanes[6] would provide new data. The passage of the rotaxane wheel over the stoppers at the ends of the axles would depend much on the size relationship between the inner wheel diameter and the outer boundaries of the stopper.[7,8] Consequently, with the same wheel, a larger stopper should slip through the wheel more slowly compared with a smaller analogue and, vice versa, a wheel with a larger diameter should pass the stopper more quickly.

[a] Kekulé-Institut für Organische Chemie und Biochemie der Universität
Gerhard-Domagk-Str. 1, 53121 Bonn, Germany
E-mail: c.schalley@uni-bonn.de

Indeed, there are several examples of the deslipping process being highly sensitive to subtle changes in the rotaxane structure. The "all-or-nothing" effect described and explained by Raymo, Houk and Stoddart is an early example:[9] Omitting just one of the nine methyl groups of a tris(*tert*-butyl)trityl stopper governs whether the rotaxane survives or the free components are liberated quickly. A stopper with three *tert*-butyl groups makes the rotaxane stable at room temperature, while one isopropyl group is sufficient to let it deslip. This finding was explained by invoking a two step process in which the barrier of the rate determining step depends much on the presence of the *tert*-butyl groups. Other studies presented evidence that many different effects influence the deslipping reaction: (a) the dynamic nature of the rotaxane is an important issue. Rotaxanes with dendritic stoppers deslip more easily than their counterparts bearing trityl stoppers, although the static model of the dendron suggests that it is much larger than the rigid trityl group.[10] The dendritic stopper is possibly capable of deslipping in a branch-by-branch fashion. (b) Flexibility has a marked influence. The lower rotational barrier of sulfonamide versus carboxamide groups in the wheel reduces the half life of otherwise identical rotaxanes by a factor of about 100.[11] (c) Non-covalent bonding may provoke even larger differences. When intramolecular hydrogen bonding reduces the diameter of the wheel, the half-life of the rotaxane increases by a factor of about 10,000 (Scheme 1).[11] (d) Even isotopic substitution at the stopper periphery has a distinct effect.[12] Due to the lower vibrational amplitude of the C−D bond, deuterium substitution increases the rate of deslipping by ca. 10 % resulting in an inverse, secondary kinetic isotope effect of KIE =

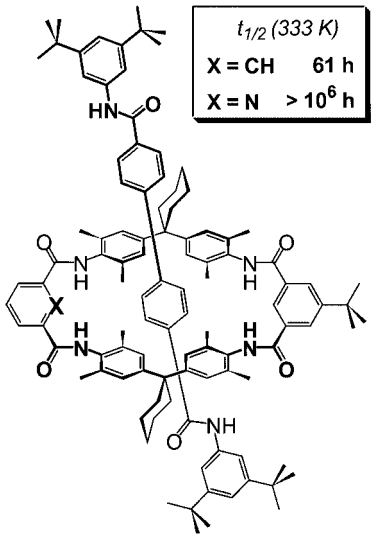

Scheme 1. Two rotaxanes which differ only with respect to the part marked "X". Introduction of a pyridine nitrogen atom instead of an isoelectronic CH increases the half life by a factor of more than 10,000

0.9.[13] It is this result in particular which clearly demonstrates how sensitive the deslipping process is to subtle changes in the rotaxane structure.

One question arises from these results: is it reasonable to describe all these effects as steric in nature? This question stands in direct relation to the problems discussed above when considering the definition of "steric effect". Here, we present another case which provokes even more severe doubt. The rotaxanes **2@1** and **6@1** compared in this study (Scheme 2) are identical with the exception of the orientation of the ester groups connecting the stoppers to the axle center piece. Despite this small structural change, we have found drastic differences in the deslipping rates for the two rotaxanes which are confirmed by the other rotaxanes shown in Scheme 2 and can be explained by the cooperative interaction of hydrogen bonding between the wheel and axle and different rotational barriers at the point of stopper attachment.

Results and Discussion

Synthesis of Ester Rotaxanes: The rotaxanes **2@1−6@1** were synthesized using the Vögtle anion template effect (Scheme 3).[14] For the synthesis of **2@1**, the hydroxy-substituted semi-axle **10** becomes deprotonated and then binds within the cavity of the wheel by two strong hydrogen bonds to the amide protons of the tetralactam macrocycle. The anion-wheel complex **10@1** can then be reacted with 3,5-di(*tert*-butyl)benzoyl chloride as the second stopper. After attaching both stoppers, the rotaxane is stable at room temperature and can be easily purified by chromatography on silica gel. Rotaxanes **3@1−5@1** can be synthesized analogously using the corresponding center piece diol instead of **10**. For the synthesis of **6@1**, a slightly modified strategy may be applied that employs the 3,5-di-(*tert*-butyl)phenol as the stopper and the biphenyl-4,4′-dicarbonyl dichloride as the center piece. Again, the phenol forms a complex with the wheel after deprotonation, and two subsequent reaction steps on both sides of the center piece give rise to the rotaxane. Rotaxanes **7@1−9@1** have been described in an earlier study[11] and are included here for comparison.

Evidence for the mechanically bound structure was obtained from ^{1}H NMR spectroscopy and mass spectrometry. The protons of the axle center pieces experience the anisotropy of the aromatic rings incorporated into the macrocyclic wheel. This gives rise to large upfield shifts of the corresponding NMR signals (see below). In the MALDI mass spectra, intense signals can be seen for the rotaxane which has become charged by attachment of a proton, a sodium, or a potassium ion. Conversely, a mixture of wheel and axle does not give rise to signals at these *m*/*z* ratios. This indicates that the signals observed for the rotaxanes are not due to proton or alkali bridged dimers of axle and wheel but, rather, correspond to the mechanically bound compound. Some deslipping and/or cleavage of the ester bonds occurs either during the ionization process or in the gas phase, so that signals of low intensity for the wheel and the axle are typically observed.

Kinetic Measurements: The deslipping reaction can be easily monitored by ^{1}H NMR kinetic experiments. In the ^{1}H NMR spectra decreasing signals for the rotaxanes were found, while the signals for the free components increased. In particular, the protons of the axle center pieces strongly sense the anisotropies of the aromatic rings incorporated within the wheel and thus appear significantly shifted to higher field compared with the signals of the free axle. The chemical shifts of most other rotaxane signals also differ from those obtained for the free components but as observed before, the maximum effect was found for the axle center piece protons.[11,12] Integration of signals that are not superimposed on others allows calculation of the amount of rotaxane consumed in the deslipping reaction after each time interval. From the slope of a plot of $\ln(c/c_0)$ over t, the rate constants k at each temperature can be calculated (Figure 1, a). Arrhenius and Eyring plots (Figure 1, b,c) then provide the activation parameters E_A and A or $\Delta H^‡$ and $\Delta S^‡$, respectively.[15]

The half lives given in Table 1 clearly show that the two isomeric rotaxanes **2@1** and **6@1** both deslip, but at different rates. We aimed to study the potential solvent effects on the deslipping rates and thus compared DMSO with the less polar and much less competitive tetrachloroethane. To our surprise, **6@1** showed efficient deslippage, while the ^{1}H NMR spectrum of **2@1** did not change at all (Figure 2). While two thirds of **6@1** had dissociated into the free components after ca. 150 min, the spectrum of **2@1** showed no significant changes even after prolonged heating at 393 K for 200 h (= 12,000 min!). The presence of only very minor signals indicates that very low amounts of products were observed which most likely correspond to the products of a decomposition of the axle rather than deslippage. These signals, however, represent less than 2 % of the starting material so that more than 98 % of the rotaxane was still intact

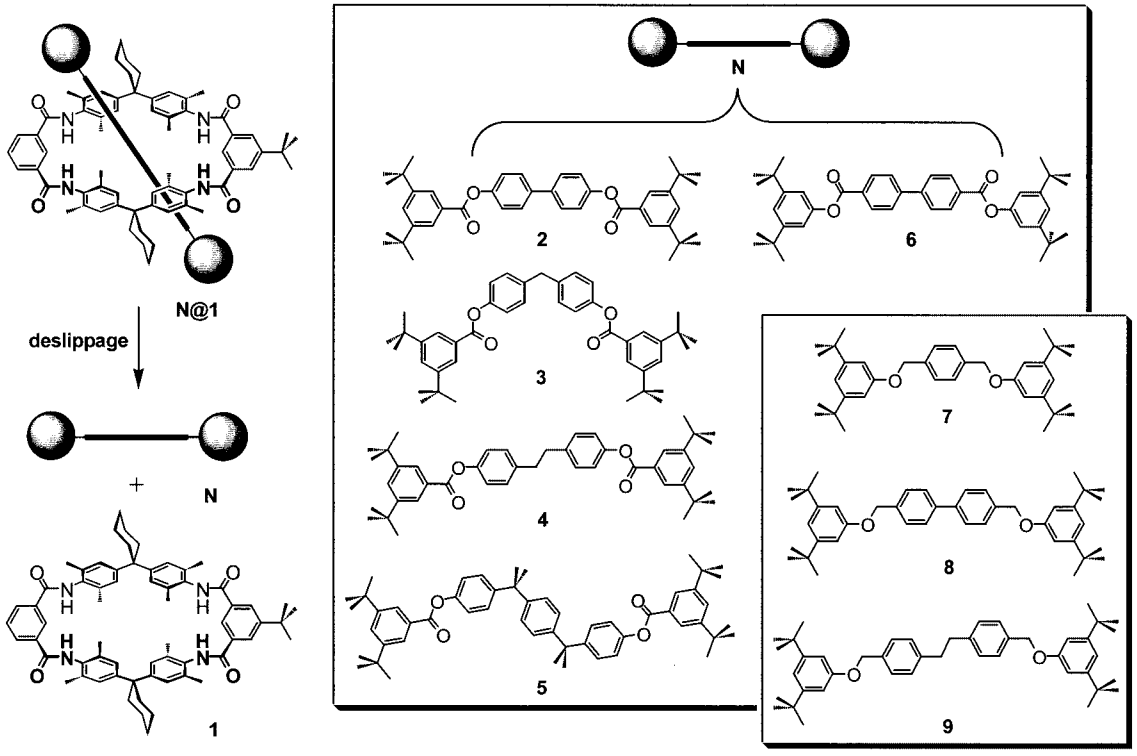

Scheme 2. Left: Schematic representation of the deslipping reaction of rotaxanes with tetralactam wheels. Right: Series of axles **2**−**6** with ester groups. Rotaxanes **7@1**−**9@1** have been studied earlier[11] and are included here for comparison

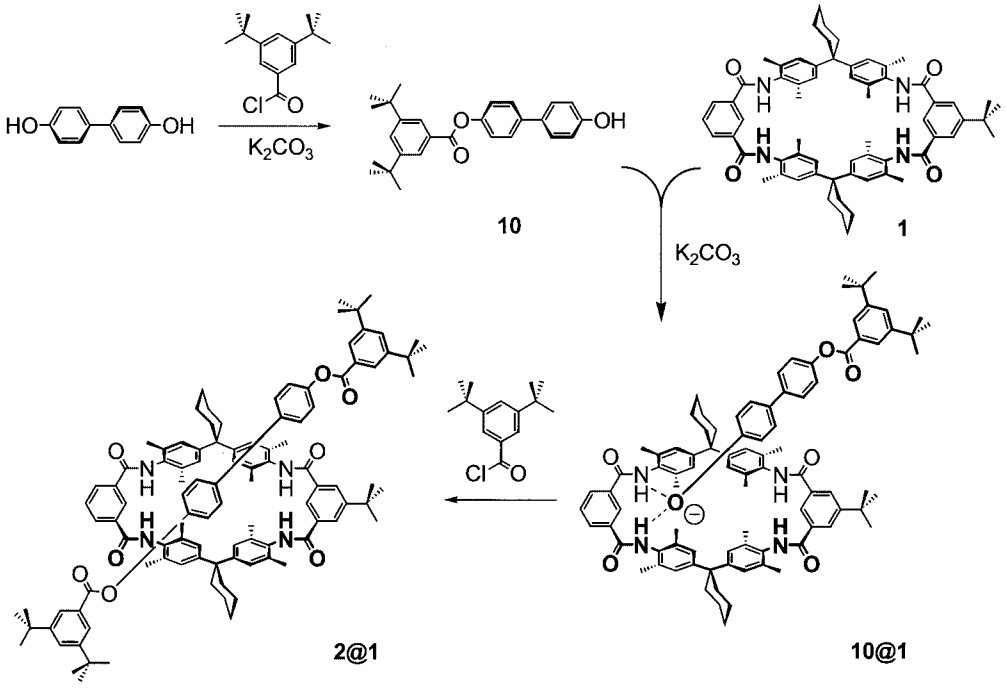

Scheme 3. Synthesis of rotaxane **2@1** by an anion template method

after heating the sample at 393 K for 200 h. This was confirmed by a MALDI mass spectrum which contained intense signals for the intact rotaxane. The same behavior was observed for rotaxanes **3@1**−**5@1**. We have therefore decided against explicitly showing the detailed NMR spectroscopic data of the whole series here and will discuss most of the results using the **2@1**/**6@1** pair of rotaxanes. Since the temperature range of tetrachloroethane is limited by its boiling point of 143 °C even in sealed NMR tubes, it was not possible to measure the full kinetic data for **2@1**−**5@1**

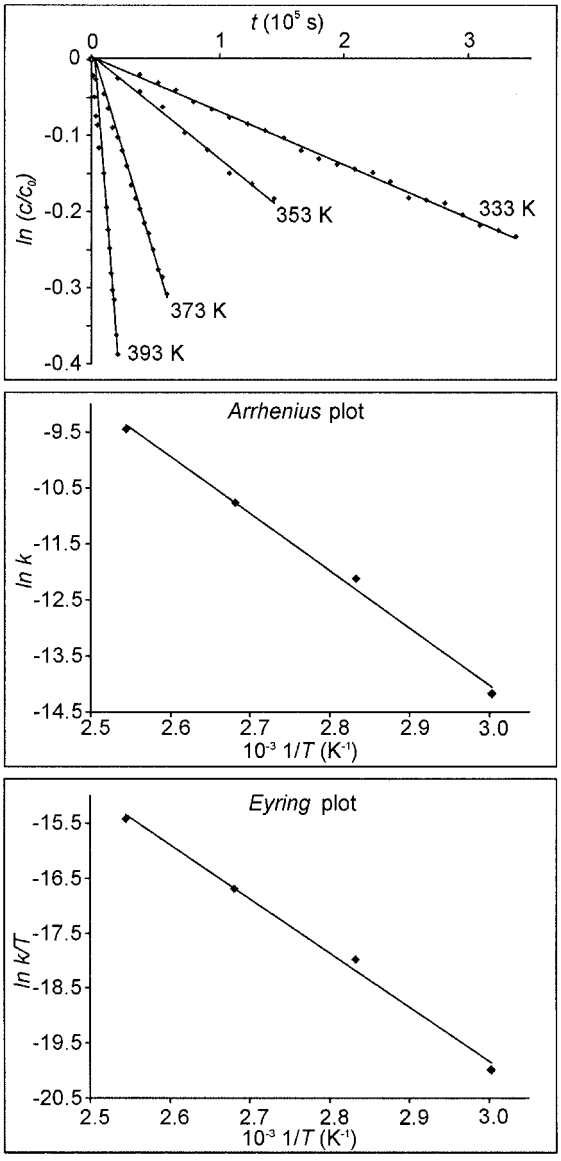

Figure 1. Deslipping of **2@1** in [D_6]DMSO: Plot of $\ln(c/c_0)$ versus t for the determination of unimolecular rate constants k at different temperatures (top). Arrhenius and Eyring plots for the determination of the activation parameters (center and bottom)

in this solvent. Consequently, we observed two different, but distinct effects: (a) The difference in structure, i.e. the orientation of the two ester groups in the axles, causes different deslipping rates in both solvents investigated here. In both cases, **2@1** deslipped more slowly than **6@1**. Thus, the rotaxane structure itself provokes different deslipping behavior. This is true even though the only change is at one of the thinnest parts of the axle, while one would expect to see an influence on the rate determining step only when the thickest part, i.e. the stopper, is altered. (b) The solvent change has a marginal effect on the deslipping of **6@1**. The half life at 373 K changes from 14 h in DMSO to 10 h in TCE (Table 1). The deslippage of **2@1**, however, is extremely dependent on the nature of the solvent. While the half life at 373 K is ca. 560 h in DMSO, it is increased to more than 25,000 h in TCE. Obviously, there is a marked solvent effect for only one of the rotaxanes despite of their close structural similarity.

A closer look at the activation parameters listed in Table 1 shows most of the activation entropies to be negative. This is indeed expected for a system which is quite flexible in its local minima on the potential energy surface, but becomes severely restricted in its mobility in the transition structure. Not only the movements of the wheel along the axle are infeasible in the transition structure but we can also safely assume[12] that quite a number of molecular vibrations and rotations have to be frozen at this point.

In DMSO, **2@1** deslips more slowly than **6@1** and this effect is largely entropic in nature. While the activation enthalpies are the same within the limits of experimental error (**2@1**: 84 kJ/mol; **6@1**: 88 kJ/mol), the entropies of activation differ significantly (**2@1**: −146 J/mol K; **6@1**: −104 J/mol·K). Changes in the activation entropy are, inter alia, connected to the flexibility of the molecule.[11] Consequently, a reasonable explanation for the difference in deslipping rates of the two rotaxanes in DMSO would be different rotational barriers at the point of stopper attachment to the axle center piece. While in **2@1** the carbonyl group is conjugated with the aromatic ring of the stopper, it is bound to the axle center piece in **6@1**. Thus, rotation around the stopper-carbonyl C−C single bond in **2@1** is hampered by a higher rotational barrier caused by conjugation of the π-systems. This is not the case in **6@1**. Flexibility at this point is thus reduced in **2@1** compared with in **6@1** and this difference translates into a slower deslippage of **2@1**. This flexibility argument is supported by the observation that rotaxanes **7@1**−**9@1** also quickly deslip. These rotaxanes also bear a flexible C−O single bond between the aromatic ring of the stopper and the axle center piece and thus resemble **6@1** in this respect.[11] Indeed, they deslip even more quickly than **6@1** in tetrachloroethane with half lives of around 1 hour or less at 373 K. This is in excellent agreement with the idea that flexibility governs the deslipping reaction here, because the ether connection of the stopper with its $-O-CH_2-$ group is again more flexible than the ester group in which the carbonyl group is attached to the center piece. Much more favorable activation entropies are found and flexibility is once again related to an entropic change.

The second effect is the huge solvent dependence of the deslipping of **2@1**. The two solvents included in this study differ with respect to their polarity and in particular to their ability to form hydrogen bonds. While DMSO is an excellent hydrogen bond acceptor, tetrachloroethane is at best a very weak one. Consequently, in tetrachloroethane, the amide protons of the wheel are more likely to form hydrogen bonds to the ester carbonyl groups of the axle. In contrast, DMSO may provoke a change of conformation in the wheel. DMSO is not only a better hydrogen bond acceptor than the ester carbonyl groups, but is also present in great

Table 1. Activation parameters obtained from an evaluation of the kinetic data using Arrhenius (E_A, A) and Eyring ($\Delta H^{\ddagger}$, $\Delta S^{\ddagger}$) plots and half lives of the rotaxanes at 373 K

	E_A [kJ·mol^{-1}]	A [MHz]	$\Delta G^{\ddagger}$ [a] [kJ·mol^{-1}]	$\Delta H^{\ddagger}$ [kJ·mol^{-1}]	$\Delta S^{\ddagger}$ [J K^{-1}·mol^{-1}]	$t_{1/2}$(373 K) [h]
2@1 [b]	87	1	128	84	−146	560
2@1 [c]	— [d]	— [d]	— [d]	— [d]	— [d]	> 25,000
3@1 [b]	101	41	130	97	−110	650
4@1 [b]	98	47	126	94	−109	220
5@1 [b]	106	328	130	102	−93	410
6@1 [b]	91	78	118	88	−104	14
6@1 [c]	85	16	116	82	−117	10
7@1 [e]	104	48300	96	101	18	1.5
8@1 [e]	98	12050	93	95	7	0.8
9@1 [e]	88	1530	88	85	−10	0.3

[a] Calculated from $\Delta H^{\ddagger}$ and $\Delta S^{\ddagger}$ at a temperature of 298 K. [b] [D_6]DMSO. [c] [D_2]Tetrachloroethane. [d] Values could not be determined due to limitations of the temperature range of TCE (see text). [e] Data taken from ref.[11], solvent: [D_2]tetrachloroethane.

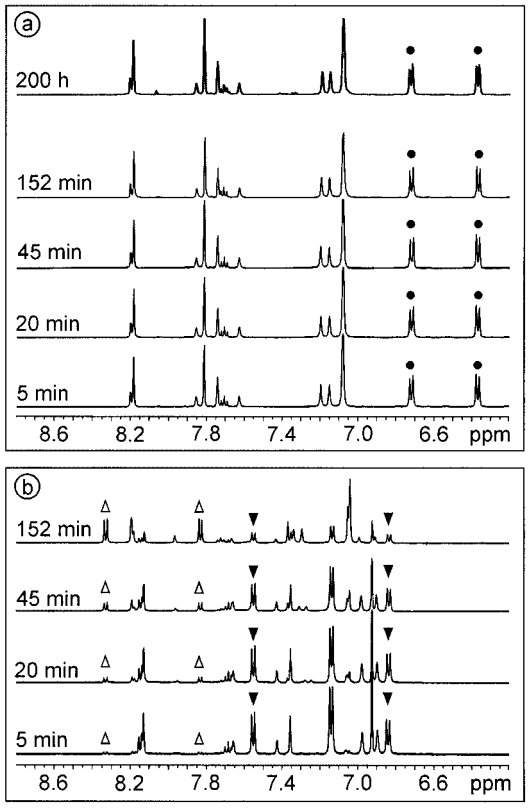

Figure 2. (a) ^{1}H NMR spectra of **2@1** after different time intervals at 393 K in tetrachloroethane. No deslipping was observed even after 200 h (top trace). Dots mark the signals for protons of the biphenyl axle center piece. (b) ^{1}H NMR spectra of **6@1** after the same time intervals and temperature in tetrachloroethane. Filled triangles denote the decreasing signals for the protons of the axle center piece of the rotaxane. Open triangles indicate growing signals of the center piece of the free axle. After 150 min, about two thirds of the rotaxane have deslipped liberating the free components.

excess and competes efficiently with the ester carbonyl groups for hydrogen bonding with the wheel amide protons. This scenario permits us to understand easily, why **2@1** deslips so much more quickly in DMSO, where the interactions between the wheel and axle are significantly reduced.

However, any explanation of the solvent effect on the deslippage of **2@1** also needs to be able to rationalize why no such drastic change of behavior was observed for **6@1**. Since the wheel is able to form a similar set of hydrogen bonds to the ester groups of **6@1**, it is not a priori clear why the two rotaxanes differ so much. We are inclined to favor the following situation which is in agreement with the experimental facts and with the molecular modeling results described below. Let us assume that both effects, i.e. the higher rotational barrier around the stopper-carbonyl bond in **2@1** and the differences in hydrogen bonding ability of the solvents, cooperate jointly. Then, in tetrachloroethane, hydrogen bonding between the wheel and the ester carbonyl groups in **2@1** automatically adjusts the stopper to be in an arrangement coplanar with the ester carbonyl group. This reduces the freedom of the stopper to orientate itself into a position favorable for deslippage. In contrast, a competitive solvent such as DMSO breaks these hydrogen bonds and liberates the axle to move into any orientation which is favorable for deslippage. These assumptions are thus in line with the huge difference in the rates of the deslipping reaction of **2@1**. For **6@1**, the situation is different. Regardless of whether hydrogen bonding between the wheel and axle occurs, the stopper is free to rotate and can thus be orientated into a favorable geometry almost independent of the solvent. Consequently, one would expect to find only a small difference in the deslipping rates for the two solvents examined here. Finally, the differences between **2@1** and **6@1** in DMSO can easily be rationalized by the changes in rigidity as outlined above. In summary, this model of a cooperative interplay of the two effects provides a reasonable explanation for the experimental results. Other scenarios, e.g. those involving different modes of hydrogen bonding can be excluded based on the following calculations.

Molecular Modeling: In order to get a more profound insight into the structural features of the rotaxanes under study and to test our hypothesis in some detail, **2@1** and **6@1** and their components were studied by computational methods. One of the problems associated with the mol-

ecules studied here is their size and consequently their large conformational space. A two step procedure was therefore applied. First, favorable conformations were sought using a 4000 step Monte Carlo simulation with the Amber* force field[16] implemented in MacroModel 8.0.[17] Several starting geometries were used and in particular, potential conformations with a high number of hydrogen bonds between axle and wheel were carefully sought. The most favorable conformations were then grouped into families with similar structural features and from each of these families the most favorable conformation was re-optimized at the AM1 level of theory using the MOPAC version provided with the CaChe 5.0 program package.[18] Qualitatively, these calculations are in agreement with the results obtained by the force field calculations so that we will restrict the following discussion to the AM1 structures.

A second problem is that we were dealing with a kinetic study. Consequently, transition structures should be discussed rather than local minima on the potential energy surface. However, for molecules as large as the rotaxanes under study here, it is difficult to find the transition structures by conventional means such as semi-empirical methods.[9,19] In particular, the high degree of flexibility of the mechanical bond is problematic. For these reasons, we have refrained from making quantitative statements in the following discussion, but regard the calculations merely as a qualitative tool to test some of the conjectures made above.

At first, the properties of the free components, i.e. axle and wheel, need to be discussed briefly. The two axles **2** and **6** are shown in Figure 3 superimposed on their electrostatic potential surfaces. Quite clearly, the geometric features are almost the same. The distances between the two carbonyl oxygen atoms differ only by 0.5 Å. Also, the electrostatic potential surfaces are quite similar. The differences are mostly due to the electron-withdrawing properties of the carbonyl group which make the attached aromatic ring more positive. Even if one attempts to correlate the differences found in the calculations with the experimentally observed deslipping behavior, it is not quite clear how they are connected with each other in detail. For both stoppers, the rotational barriers have been calculated at the AM1 level of theory by mapping the dihedral angles of the model compound shown in Figure 4 between 0° and 180° in steps of 1°. In each step, the dihedral angle was constrained, while all other parts of the molecule were geometry-optimized. The difference between both rotational barriers amounts to ca. 8−9 kJ/mol.

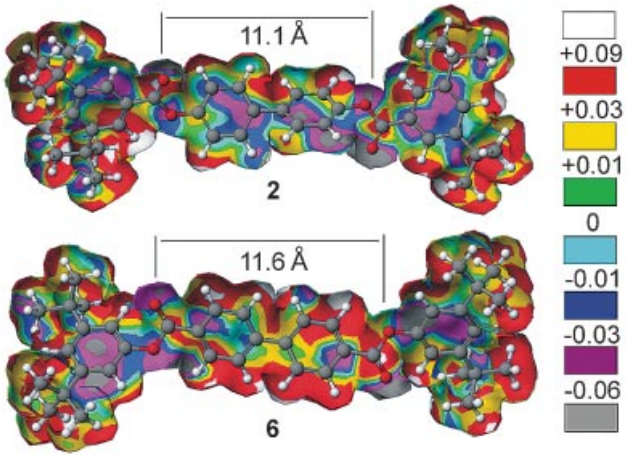

Figure 3. AM1-optimized conformations of axles **2** and **6**. The distance between the two carbonyl groups is given above each structure. The color code corresponds to the electrostatic potential surface. It is defined as shown in the legend on the right. The numbers are given in atomic units (0.01 a.u. corresponds to ca. 25 kJ/mol) and represent the attraction between the molecule surface and a point charge located at a distance of 1 Å above the surface at the border between two differently colored areas

As far as the wheel is concerned, two questions are of major importance in the context of the kinetic results presented here: (i) The overall shape of the wheel's most favorable conformations may give an idea as to how the deslipping might proceed. Thus, the first question is: How large is the inner cavity of the wheel? (ii) If hydrogen bonding to DMSO is possible, the amide hydrogen atoms must be able to turn outwards without causing unfavorable energy changes. Since the cavity of the rotaxane wheel is more or less fully occupied by the axle, there is no room for the DMSO molecules to enter the cavity and to form hydrogen bonds with a favorable geometrical arrangement inside. Thus the second question is: How much energy is needed to turn the amide protons to the outside of the wheel? The most favorable conformations of the wheel obtained from computer modeling are depicted in Figure 5. Indeed, several conformations exist which differ from each other with respect to the in/out orientation of the amide NH hydrogen atoms. Although we were unable to locate a structure with all four amides in their out-conformation, the three structures shown in Figure 4 are all energetically within 2 kJ/mol even without any solvent present. These differences are too small for us to be sure which of the structures is the most favorable. Consequently, it is likely that the amide groups are able to turn outwards in order to form hydrogen bonds with a solvent such as DMSO with its excellent hydrogen bond acceptor qualities. The energetic costs of these changes are easily overcome by the binding energies of the newly formed hydrogen bonds. The other aspect is the overall size of the cavity. In Figure 5, the distances between the two spiro centers and between the two inner isophthalic acid hydrogen atoms are given as a measure of the cavity sizes. It is clear that the long axis of the cavity spans between the two spiro centers. Even if one argues that other parameters (such as the distance between the two carbons next to the spiro centers and the distance between the C-2 positions of the isophthalic acid) should be used, this argument does not change qualitatively. Consequently, it seems likely that the deslipping process will be more favorable when the stopper is co-linear to the line between the two spiro centers.

Finally, the structures obtained for the two rotaxanes **2@1** and **6@1** (Figure 6) shall be discussed. Both rotaxanes form only one bifurcated hydrogen bond between the axle and the wheel in their most favorable geometries. For **2@1**

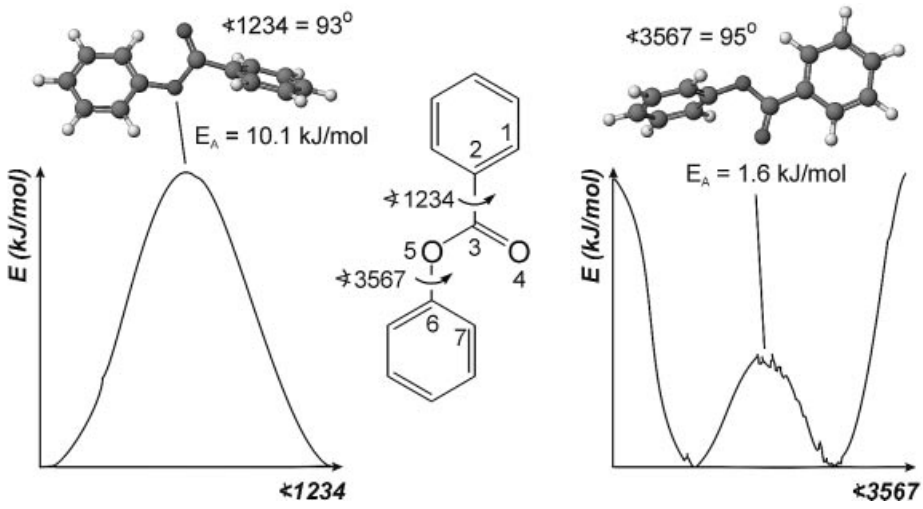

Figure 4. Dihedral angles (in degrees) of the model compound used for calculation of the two rotational barriers by mapping both angles between 0° and 180° in steps of 1° at the AM1 level. The graphs show the corresponding potential energy curves

we were unable to locate any conformation with more than this, but for **6@1** a conformation was found in which both ester carbonyl groups were involved in hydrogen bonding. Each of them formed one hydrogen bond with one of the amide protons of each isophthalic carboxamide group of the wheel. However, this conformation requires a significant distortion of the wheel from its most favorable geometry and this conformation is therefore higher in energy than that shown in Figure 6 by ca. 45 kJ/mol and can be ruled out as the major equilibrium conformation. The energy differences for in/out conformers of the isophthalic carboxamides not involved in hydrogen bonding are again small and all-in conformations have similar energies as in/in/in/out conformations. The most interesting aspect of the two structures, however, is the different orientation of the stopper groups next to the hydrogen-bonded carbonyl group. For **2@1**, the stopper is coplanar with the carbonyl group, while it is oriented orthogonal to the carbonyl group in **6@1**. A second conformer could be found for the latter rotaxane in which the stopper is coplanar with the carbonyl group which is higher in energy by ca. 9 kJ/mol. For **2@1**, however, we were unable to locate a minimum in which the stopper is arranged in an orthogonal fashion with respect to the carbonyl group.

These calculations allow us to draw the following conclusions: (i) The two axles **2** and **6** are similar to each other, in particular with respect to the fact that they both form hydrogen bonds between the wheel and only one of the ester carbonyl groups. (ii) In tetrachloroethane, hydrogen bonding can be expected to involve two adjacent amide groups of the wheel and one of the ester carbonyl groups of the axle in a bifurcated arrangement. The axles of all rotaxanes under study are too long to allow the formation of additional hydrogen bonds involving the other amides or the other ester group. (iii) The rotational barriers calculated for a model compound differ by ca. 10 kJ/mol. This value is likely to be higher in the rotaxane where the methyl groups incorporated in the wheel hamper stopper rotation additionally. The stopper of **2@1** is more deeply inserted into the cavity due to the lack of the additional oxygen atom between the carbonyl group and stopper as in **6@1**. (iv) Interchange of in- and out-conformers of the wheel's amide groups is possible without significant energy changes. Thus, DMSO as a competitive solvent may well compete with the axle carbonyl groups for hydrogen bonding by inducing a turn of the amide groups. These conformational changes easily account for the small difference observed in the deslipping behavior of **6@1** in DMSO versus TCE. (v) The cavity of the wheel extends more between the two spiro centers than between the two isophthalic acid moieties. (vi) The preferred orientation of the stopper is coplanar with the proximal carbonyl group in **2@1** and is more likely to be vertical to that for **6@1**. Consequently, the arrangement in **6@1** appears to be better pre-organized for deslippage than that in **2@1**. The results from molecular modeling are thus consistent with both the experimental results and our interpretation in terms of a coupled interplay of rotational barriers and hydrogen bonding.

Conclusions

The experiments and calculations described here provide insight into the dynamic features of the rotaxanes under study. The surprisingly large effects of the orientations of the ester groups in the rotaxane axles and the drastic solvent effects point to a coupled interplay of hydrogen bonding between the axle and wheel and rotational barriers at the point of stopper attachment. The cooperation of these two effects is interesting in itself from the viewpoint of basic chemical research since these results shed light on the classical problem of steric effects from a new, supramolecular perspective. Although an intuitive concept of enormous utility, it is rather difficult to provide an exact definition of the term "steric size". A definition based on van der Waals radii does definitively not explain the experimental findings

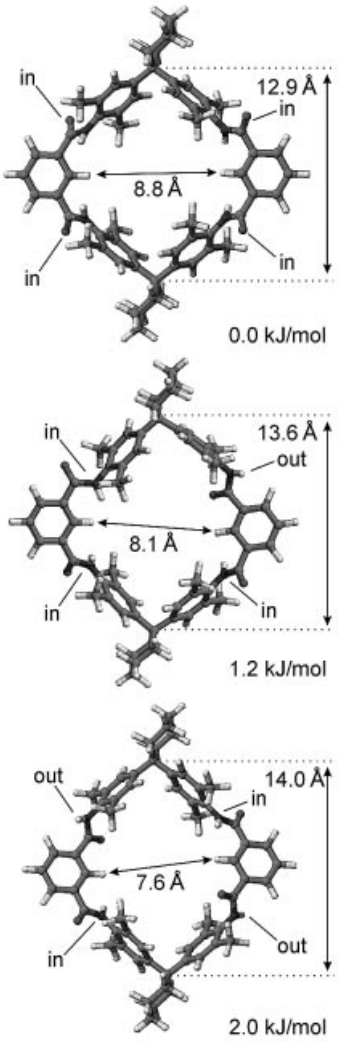

Figure 5. Different AM1-optimized conformations of the tetralactam macrocycle and the dimensions of the cavity given as distances of the two spiro centers in the vertical and of the two inner isophthalic acid hydrogen atoms in the horizontal direction. Despite the rigidity of the aromatic rings, the macrocycle can adopt different conformations as far as the amide groups (in/out) are concerned. The energy differences are within 2 kJ/mol and can thus be regarded as equal for all the conformations

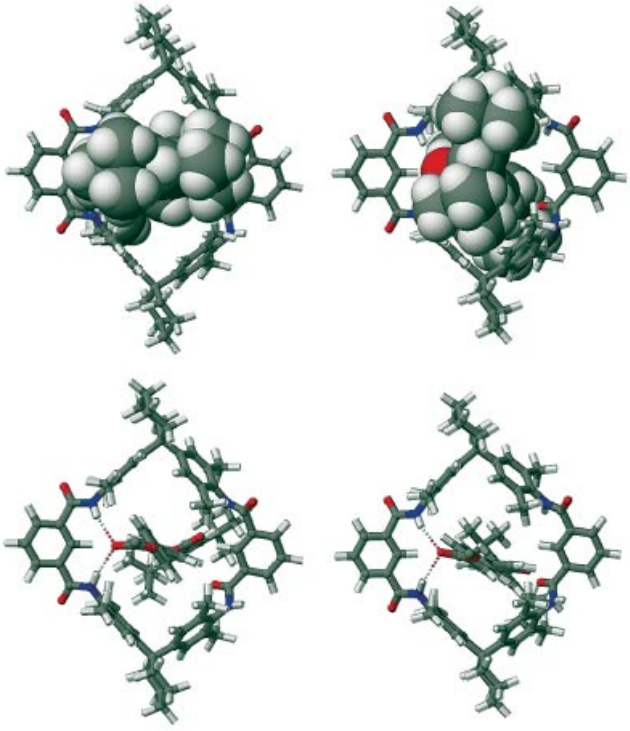

Figure 6. AM1-optimized lowest energy conformations of **2@1** (left) and **6@1** (right). Both rotaxanes are shown as top views. Top: For clarity, the stopper is shown in a space filling representation and the wheel as stick model (*tert*-butyl groups omitted). The pictures at the bottom show the rotaxane with the frontal stopper omitted in order to permit an unobstructed view of the hydrogen bonding pattern. Note that in both cases the axles are too long to permit the formation of more than two hydrogen bonds to the amide protons of the wheel

presented here. One might thus argue that the enthalpy of activation is more or less the same for both rotaxanes **2@1** and **6@1**. Using the definition of steric effects as the enthalpic contribution to an activation barrier, one would arrive at the conclusion that the observed effects are not steric in nature because the most significant change is observed in the entropy of activation. However, this would then also hold true for the steric isotope effect observed earlier[12] which is due to a change in vibrational amplitude and was found to be predominantly entropic in nature. Also, it is not clear why the other rotaxanes included in this study show the observed enthalpy−entropy compensation although they merely bear different axle center pieces while the stoppers are the same for all. One would rather expect that they do not differ much in their steric demands and that all rotaxanes have the same enthalpy of activation for the deslipping reaction. This is not the case however. Consequently, this study questions the concept of steric size and points to some of its difficulties and limitations.

Another aspect of potentially even greater future importance should be mentioned: Natural molecular machines such as the ATP synthase enzyme complex[20] and many others represent a class of extremely efficient devices. One reason why nature uses very complex structures for implementing function may be that a complex system can be fine tuned and thus optimized by an accordingly larger number of subtle adjustments in structure.[21] During the past decade, artificial molecular machines based on rotaxanes and catenanes[22] have become more and more sophisticated but they are still no match at all for their natural counterparts with respect to neither complexity nor efficiency. Most of the systems referred to in the literature as "machines" are not even fully functional models of their macroscopic analogues. We have no doubt, however, that artificial molecular motors and other nano-devices will finally be realized by supramolecular chemists. A detailed understanding of effects such as those reported here may then become an important tool for their design. In particular, the fine tuning of the properties of such machines will probably rely on and make use of these and other subtle structural variations in order to improve their performance and optimize their efficiency. The example of the ester rot-

axanes provides an approach to significant changes in their properties without large structural changes which would possibly have unwanted side effects.

Experimental Section

Kinetic Studies: For each of the rotaxanes, the rate constants of the deslipping reaction were measured at several different temperatures by ^{1}H NMR experiments. In preliminary experiments, the temperature range was chosen such that deslipping occurred with a reasonable half life. The NMR samples were kept in an oil bath at constant temperature. When the half life was short enough at temperatures accessible with the NMR instrument's heater, the samples were kept in the NMR spectrometer instead. In each experiment, the deslipping was followed until at least 75 % of the rotaxane had been consumed or until one of the free components precipitated from the NMR solution, whichever occurred first. For the evaluation of the data, the integrals of several signals were averaged wherever possible in order to reduce experimental error. However, some of the rotaxanes exhibit NMR spectra in which decreasing and increasing signals overlap to such an extend that only one or two of the signals could be confidently evaluated. The estimated experimental error range was ± 4 kJ/mol for E_A and $\Delta H^‡$. Due to the logarithmic plots, the error of A and $\Delta S^‡$ was somewhat larger and we estimated it to be ± 30 % for A and $\Delta S^‡$. The Arrhenius activation parameters were derived from a plot of ln k versus $1/T$ whilst ln (k/T) was plotted versus $1/T$ in order to determine $\Delta H^‡$ and $\Delta S^‡$ according to the Eyring equation. A close inspection of the signals increasing over time confirmed that they correspond to the intact free components and thus exclude decomposition of the axle or wheel rather than deslipping as the reason for rotaxane degradation.

Molecular Modeling: The calculated structures were obtained by first performing a 3000 step Monte Carlo conformational search with the Amber* force field[16] as implemented in MacroModel 8.0.[17] The lowest energy conformers out of 3000 structures were determined by placing closure bonds in the macrocycles (one of the amide bonds) and the attached cyclohexyl side chains. While the aromatic rings and the amides were constrained to planarity, all single bonds (with the exception of those of the methyl groups) were selected to allow rotations into other conformations. For each minimization, the number of iterations was set to 10,000 in order to generate fully converged structures. The energy range for structures for storage in the output file was set to 50 kJ/mol above the lowest energy conformer. The best conformations were then re-optimized at the AM1 level of theory as implemented in the MOPAC version provided with the CaChe 5.0 program package.[18] Electrostatic potential surfaces of the axles were also calculated with this program.

Syntheses of Rotaxanes: Wheel **1** was prepared according to well established literature procedures.[23] Threading of the axle into the wheel cavity can easily be accomplished using a recently published anion template effect.[14] The synthetic precursors for the series of ether rotaxanes were commercially available and were used without further purification. Usually, elemental analyses for macrocycles and rotaxanes are not within the typically accepted range due to varying amounts of solvents which can not be entirely removed from the samples. These solvents can easily be detected in the NMR spectra. We therefore based the characterization of the target compounds mainly on ^{1}H and ^{13}C NMR experiments and mass spectrometry. All routine NMR spectroscopic experiments were performed with 300, 400, and 500 MHz Bruker instruments; the solvent signal was used for internal calibration. Furthermore, all rotaxanes gave clean MALDI (Micromass MALDI-TofSpec-E) mass spectra with isotope patterns that agree well with those calculated on the basis of natural abundances.

Representative Procedure for the Synthesis of Rotaxanes with 3,5-Di(*tert*-butyl)benzoic Acid Stoppers: A suspension of the tetralactam macrocycle **1** (100 mg, 0.104 mmol), dibenzo[18]crown-6 (8 mg, 0.021 mmol), K_2CO_3 (29 mg, 0.208 mmol), 3,5-di(*tert*-butyl)-benzoyl dichloride (52 mg, 0.208 mmol) and 4,4′-dihydroxybiphenyl (19 mg, 0.104 mmol) was prepared under argon at 0 °C in dichloromethane (5 mL). The mixture was warmed to room temperature and stirred for 6 days. After filtration and evaporation of the solvent under reduced pressure, the crude product was purified by column chromatography on silica gel (40−63 μm, CH_2Cl_2/ethyl acetate, 25:1). Rotaxane **2@1** was obtained in 34 % yield (55 mg, 0.035 mmol) as a colorless solid.

Rotaxane 2@1: [2]{4,4′-Bis[3,5-di(*tert*-butyl)benzoyloxy]biphenyl}-{11′-(*tert*-butyl)-5′,17′,23′, 35′,38′,40′,43′,45′-octamethyldispiro-[cyclohexane-1,2′-7′,15′,25′,33′-tetraazaheptacyclo[32.2.2.2$^{3′.6′}$.2$^{16′.19′}$.2$^{21′.24′}$.1$^{9′.13′}$.1$^{27′.31′}$]hexatetraconta-3′,5′,9′,11′,13′(44′),16′,18′, 21′,23′,27′,29′,31′(39′),34′,36′,37′,40′,42′,45′-octadecaene-20′,1′′-cyclohexane]-8′,14′,26′,32′-tetrone}rotaxane: Yield 34 %; R_f (CH_2Cl_2/ethyl acetate, 25:1) = 0.43; m.p. 233−235 °C. ^{1}H NMR (400 MHz, $C_2D_2Cl_4$): δ = 1.24 (s, 36 H, stopper-*t*Bu), 1.35 (s, 9 H, wheel-*t*Bu), 1.50 (s, 4 H, cyhex), 1.65 (s, 8 H, cyhex), 1.85 (s, 12 H, Ar-CH_3), 1.86 (s, 12 H, Ar-CH_3), 2.31 (s, 8 H, cyhex), 6.29 (d, ^3J = 8.6 Hz, 4 H, biphenyl), 6.63 (d, ^3J = 8.6 Hz, 4 H, biphenyl), 7.00 (s, 8 H, Ar-H), 7.08 (s, 2 H, NH), 7.13 (s, 2 H, NH), 7.55 (s, 1 H, Ar-H, wheel), 7.62 (t, ^3J = 7.7 Hz, 1 H, Ar-H, wheel), 7.66 (s, 2 H, Ar-H, stopper), 7.74 (s, 4 H, Ar-H, stopper), 7.78 (s, 1 H, Ar-H, wheel), 8.09−8.11 (m, 4 H, Ar-H, wheel) ppm. ^{13}C NMR (100 MHz, $C_2D_2Cl_4$): δ = 18.4, 18.6, 23.0, 26.2, 31.1, 34.8, 35.2, 35.8, 45.2, 122.2, 124.02, 126.5, 126.7, 126.8, 127.5, 128.8, 130.9, 131.1, 131.9, 134.3, 134.4, 135.1, 136.5, 149.01, 150.16, 151.8, 154.0, 164.6, 165.1, 167.5 ppm. MALDI-TOF-MS ($C_{106}H_{122}N_4O_8$): m/z = 1580.7 [M + H$^+$], 1602.7 [M + Na$^+$], 1618.6 [M + K$^+$].

Rotaxane 3@1: [2]{1,1-Bis-[3,5-di-*tert*-butylbenzoyloxy-phenyl]-methane}-{11′-(*tert*-butyl)-5′,17′,23′,35′,38′,40′,43′,45′-octamethyl-dispiro[cyclohexane-1,2′-7′,15′,25′,33′-tetraazaheptacyclo-[32.2.2.2$^{3′.6′}$.2$^{16′.19′}$.2$^{21′.24′}$.1$^{9′.13′}$.1$^{27′.31′}$]hexatetraconta-3′,5′, 9′,11′, 13′(44′),16′,18′,21′,23′,27′,29′,31′(39′),34′,36′,37′,40′, 42′,45′octadecaene-20′,1′′-cyclohexane]-8′,14′,26′, 32′-tetrone}-rotaxane: Yield 33 %; R_f (CH_2Cl_2/ethyl acetate, 25:1) = 0.41; m.p. 195−197 °C. ^{1}H NMR (400 MHz, $C_2D_2Cl_4$): δ = 1.20 (s, 36 H, stopper-*t*Bu), 1.29 (s, 9 H, wheel-*t*Bu), 1.49 (s, 4 H, cyhex), 1.64 (s, 8 H, cyhex), 1.84 (s, 12 H, Ar-CH_3), 1.87 (s, 12 H, Ar-CH_3), 2.28 (s, 8 H, cyhex), 3.79 (s, 2 H, CH_2-ax), 5.93 (d, ^3J = 8.3 Hz, 4 H, axle), 6.53 (d, ^3J = 8.3 Hz, 4 H, axle), 6.93 (s, 4 H, Ar-H), 6.94 (s, 4 H, Ar-H), 6.96 (s, 2 H, NH), 7.12 (s, 2 H, NH), 7.59−7.63 (m, 4 H, Ar-H, wheel, stopper), 7.68 (s, 4 H, stopper), 7.91 (s, 1 H, Ar-H, wheel), 8.13−8.15 (m, 4 H, Ar-H, wheel) ppm. ^{13}C NMR (100 MHz, $C_2D_2Cl_4$): δ = 18.4, 18.5, 22.8, 22.9, 23.6, 26.2, 28.7, 30.1, 31.0, 31.9, 34.7, 35.0, 35.5, 38.5, 45.1, 68.0, 120.9, 121.7, 123.4, 123.8, 126.5, 127.5, 128.9, 130.2, 130.6, 130.7, 131.8, 132.1, 134.2, 134.3, 134.9, 135.0, 138.1, 148.8, 148.9, 148.9, 151.7, 154.0, 164.2, 164.6, 167.2, 167.5 ppm. MALDI-TOF-MS ($C_{107}H_{124}N_4O_8$): m/z = 1594.8 [M + H$^+$], 1616.8 [M + Na$^+$], 1633.7 [M + K$^+$].

Rotaxane 4@1: [2]{4,4′-Bis[3,5-di-*tert*-butylbenzoyloxy]-1,1′-bibenzyl}-{11′-*tert*-butyl-5′,17′,23′,35′,38′,40′,43′,45′-octa-

methyldispiro[cyclohexane-1,2′-7′,15′,25′,33′-tetraazaheptacyclo-[32.2.2.2$^{3',6'}$.2$^{16',19'}$.2$^{21',24'}$.1$^{9',13'}$.1$^{27',31'}$]hexatetraconta-3′,5′,9′,11′,13′(44′),16′,18′,21′,23′,27′,29′,31′(39′),34′,36′,37′,40′,42′,45′-octadecaene-20′,1′′-cyclohexane]-8′,14′,26′,32′-tetrone}-rotaxane: Yield 29 %; R_f (CH_2Cl_2/ethyl acetate, 25:1) = 0.41; m.p. 223−225 °C. ^{1}H NMR (400 MHz, $C_2D_2Cl_4$): δ = 1.21 (s, 36 H, stopper-*t*Bu), 1.26 (s, 9 H, wheel-*t*Bu), 1.49 (s, 4 H, cyhex), 1.64 (s, 8 H, cyhex), 1.81−1.87 (m, 24 H, Ar-CH_3), 2.28 (s, 8 H, cyhex), 5.87 (d, ^3J = 5.8 Hz, 4 H, axle), 6.58 (d, ^3J = 7.9 Hz, 4 H, axle), 6.91- 6.94 (m, 8 H, Ar-H, wheel), 7.09 (s, 2 H, NH), 7.13 (s, 2 H, NH), 7.55- 7.59 (m, 2 H, Ar-H, wheel), 7.64 (s, 2 H, stopper), 7.68 (s, 4 H, stopper), 7.90 (s, 1 H, Ar-H, wheel), 8.12- 8.15 (m, 4 H, Ar-H, wheel) ppm. ^{13}C NMR (100 MHz, $C_2D_2Cl_4$): δ = 18.4, 18.4, 18.5, 18.5, 22.1, 22.9, 26.2, 31.0, 31.0, 34.7, 35.0, 35.5, 43.3, 45.1, 120.8, 121.6, 123.3, 123.8, 126.5, 127.9, 128.5, 128.8, 130.2, 130.5, 130.6, 130.7, 130.7, 131.8, 134.1, 134.2, 134.2, 135.0, 143.5, 148.7, 148.8, 148.9, 149.0, 151.8, 154.0, 164.1, 164.1, 164.6, 164.7, 167.2 ppm. MALDI-TOF-MS ($C_{108}H_{126}N_4O_8$): *m*/*z* = 1607.6 [M + H^+], 1629.7 [M + Na^+], 1645.6 [M + K^+].

Rotaxane 5@1: [2]{1,4-Bis-{1-[4-(3,5-di-*tert*-butylbenzoyloxy)-phenyl]-1-methyl-ethyl}benzene}-{11′-*tert*-butyl-5′,17′,23′,35′,38′,40′,43′,45′-octamethyldispiro[cyclohexane-1,2′-7′,15′,25′,33′-tetraazaheptacyclo[32.2.2.2$^{3',6'}$.2$^{16',19'}$.2$^{21',24'}$.1$^{9',13'}$.1$^{27',31'}$]hexatetraconta-3′,5′,9′,11′,13′(44′),16′,18′,21′,23′,27′,29′,31′(39′),34′,36′,37′,40′,42′,45′-octadecaene-20′,1′′-cyclohexane]-8′,14′,26′,32′-tetrone}rotaxane: Yield 45 %; R_f (CH_2Cl_2/ethyl acetate, 25:1) = 0.56; m.p. 225−227 °C. ^{1}H NMR (500 MHz, $C_2D_2Cl_4$): δ = 1.24−1.36 (s, 36 H, stopper-*t*Bu), 1.45 (s, 9 H, wheel-*t*Bu), 1.50 (s, 12 H, axle-C(CH_3)$_2$], 1.57 (s, 4 H, cyhex), 1.65−1.70 (m, 8 H, cyhex), 1.88 (s, 24 H, Ar-CH_3), 2.36 (s, 8 H, cyhex), 6.98 (s, 8 H, Ar-H, wheel), 7.10 (s, 4 H, NH), 7.72−7.77 (m, 8 H, Ar-H, wheel, stopper), 7.96 (s, 1 H, Ar-H, wheel), 8.24 (m, 2 H, Ar-H, wheel), 8.26 (s, 2 H, Ar-H, wheel) ppm. MALDI-TOF-MS ($C_{118}H_{138}N_4O_8$): *m*/*z* = 1740.3 [M + H^+], 1762.3 [M + Na^+], 1778.3 [M + K^+].

Rotaxane 6@1: [2]{4,4′-Bis[3,5-di(*tert*-butyl)phenoxycarbonyl]-1,1′-biphenyl}-{11′-*tert*-butyl-5′,17′,23′,35′,38′,40′,43′,45′-octamethyldispiro[cyclohexane-1,2′-7′,15′,25′,33′-tetraazaheptacyclo-[32.2.2.2$^{3',6'}$.2$^{16',19'}$.2$^{21',24'}$.1$^{9',13'}$.1$^{27',31'}$]hexatetraconta-3′,5′,9′,11′,13′(44′),16′,18′,21′,23′,27′,29′,31′(39′),34′,36′,37′,40′,42′,45′-octadecaene-20′,1′′-cyclohexane]-8′,14′,26′, 32′-tetrone}rotaxane: A suspension of K_2CO_3 (29 mg, 0.208 mmol), dibenzo[18]crown-6 (8 mg, 0.021 mmol), 3,5-di(*tert*-butyl)phenol (43 mg, 0.208 mmol) and the tetralactam macrocycle **1** (100 mg, 0.104 mmol) in trichloromethane (5 mL) was stirred under argon for 20 min at 0 °C. A solution of 4,4′-biphenyldicarbonyl dichloride (29 mg, 0.104 mmol) in trichloromethane (3 mL) was then added over a period of 1.5 h and the mixture stirred for 6 days at room temperature. The mixture was then filtered, the solvent removed under reduced pressure and the crude product purified by column chromatography on silica gel (40−63 μm, CH_2Cl_2/ethyl acetate, 25:1). Rotaxane **6@1** was obtained in 15 % yield (25 mg; 0.016 mmol) as a colorless solid. R_f (CH_2Cl_2/ethyl acetate, 25:1) = 0.47; m.p. 218−220 °C. ^{1}H NMR (400 MHz, $C_2D_2Cl_4$): δ = 1.24 (s, 36 H, stopper-*t*Bu), 1.32 (s, 9 H, wheel-*t*Bu), 1.53 (s, 4 H, cyhex), 1.67 (s, 8 H, cyhex), 1.94 (s, 12 H, Ar-CH_3), 1.94 (s, 12 H, Ar-CH_3), 2.35 (s, 8 H, cyhex), 6.75 (d, ^3J = 8.3 Hz, 4 H, biphenyl), 6.78 (s, 2 H, NH), 6.85 (m, 6 H, stopper, NH), 7.05 (s, 4 H, Ar-H), 7.07 (s, 4 H, Ar-H), 7.27 (s, 2 H, stopper), 7.33 (s, 1 H, Ar-H, wheel), 7.47 (d, ^3J = 8.3 Hz, 4 H, biphenyl), 7.56 (s, 1 H, Ar-H, wheel), 7.59 (t, ^3J = 7.7 Hz, 1 H, Ar-H, wheel), 8.05- 8.07 (m, 4 H, Ar-H, wheel) ppm. ^{13}C NMR (100 MHz, $C_2D_2Cl_4$): δ = 18.7, 18.8, 22.9, 26.2, 31.0, 31.2, 34.7, 35.0, 35.6, 45.4, 114.9, 120.4, 125.9, 126.8, 126.9, 128.8, 129.4, 130.1, 130.3, 130.9, 131.0, 131.8, 134.6, 134.6, 142.5, 148.5, 148.7, 149.9, 152.5, 154.1, 164.6, 165.0, 165.1 ppm. MALDI-TOF-MS ($C_{106}H_{122}N_4O_8$): *m*/*z* = 1602.8 [M + Na^+], 1618.7 [M + K^+].

Acknowledgments

We thank Prof. Fritz Vögtle for continuous support and acknowledge funding from the Deutsche Forschungsgemeinschaft (SFB, 624) and the Fonds der Chemischen Industrie. We are particularly grateful to Claus Schmidt and Hannelore Spitz for their help with recording numerous NMR spectra.

[1] [1a] *Steric Effects in Organic Chemistry* (Ed.: M. S. Newman), Wiley, New York, **1956**. [1b]H. Förster, F. Vögtle, *Angew. Chem.* **1977**, *89*, 443; *Angew. Chem. Int. Ed. Engl.* **1977**, *16*, 429.

[2] [2a] H. A. Stuart, *Molekülstruktur*, Springer, Berlin **1967**. [2b]A. Bondi, *J. Phys. Chem.* **1964**, *68*, 441. [2c] S. C. Nyburg, J. T. Szymański, *J. Chem. Soc., Chem. Commun.* **1968**, 669.

[3] R. W. Taft, Jr., see ref.[1a], pp. 561 and 660.

[4] [4a] S. Winstein, N. J. Holness, *J. Am. Chem. Soc.* **1955**, *77*, 5562. For an overview, see: [4b] J. Hirsch, *Top. Stereochem.* **1967**, *1*, 199.

[5] M. C. T. Fyfe, F. M. Raymo, J. F. Stoddart, in *Stimulating Concepts in Chemistry* (Eds.: J. F. Stoddart, F. Vögtle), Wiley-VCH, Weinheim, **2000**, p. 211.

[6] [6a] G. Schill, *Catenanes, Rotaxanes and Knots*, Academic Press, New York, **1971**. [6b]C. O. Dietrich-Buchecker, J.-P. Sauvage, *Chem. Rev.* **1987**, *87*, 795. [6c] J.-P. Sauvage, *Acc. Chem. Res.* **1990**, *23*, 319. [6d] H. W. Gibson, H. Marand, *Adv. Mater.* **1993**, *5*, 11. [6e] R. Hoss, F. Vögtle, *Angew. Chem.* **1994**, *106*, 389; *Angew. Chem. Int. Ed. Engl.* **1994**, *33*, 375. [6f] R. Jäger, F. Vögtle, *Angew. Chem.* **1997**, *109*, 966; *Angew. Chem. Int. Ed. Engl.* **1997**, *36*, 930. [6g] S. A. Nepogodiev, J. F. Stoddart, *Chem. Rev.* **1998**, *98*, 1959. [6h] F. M. Raymo, J. F. Stoddart, *Chem. Rev.* **1999**, *99*, 1043. [6i] *Molecular Catenanes, Rotaxanes, and Knots* (Eds.: J. P. Sauvage, C. Dietrich-Buchecker), Wiley-VCH, Weinheim, **1999**. [6j]T. Takata, N. Kihara, *Rev. Heteroatom Chem.* **2000**, *22*, 197. [6k] T. J. Hubin, D. H. Busch, *Coord. Chem. Rev.* **2000**, *200*, 5. [6l] P. Linnartz, C. A. Schalley, *Rotaxanes and Pseudorotaxanes* in: *Encyclopedia of Supramolecular Chemistry* (Eds.: J. L. Atwood, J. W. Steed), Dekker, New York, in press.

[7] [7a] P. R. Ashton, R. Ballardini, V. Balzani, M. Bělohradský, M. T. Gandolfi, D. Philp, L. Prodi, F. M. Raymo, M. V. Reddington, N. Spencer, J. F. Stoddart, M. Venturi, D. J. Williams, *J. Am. Chem. Soc.* **1996**, *118*, 4931. [7b] M. Asakawa, P. R. Ashton, R. Ballardini, V. Balzani, M. Bělohradský, M. T. Gandolfi, O. Kocian, L. Prodi, F. M. Raymo, J. F. Stoddart, M. Venturi, *J. Am. Chem. Soc.* **1997**, *119*, 302. [7c] P. R. Ashton, I. Baxter, M. C. T. Fyfe, F. M. Raymo, N. Spencer, J. F. Stoddart, A. J. P. White, D. J. Williams, *J. Am. Chem. Soc.* **1998**, *120*, 2297. For a review, see: M. C. T. Fyfe, F. M. Raymo, J. F. Stoddart, *Slippage and Constrictive Binding*, in *Stimulating Concepts in Chemistry* (Eds.: F. Vögtle, J. F. Stoddart, M. Shibasaki), Wiley-VCH, Weinheim **2000**.

[8] This holds also true for the slipping synthesis of rotaxanes. See, for example: [8a] I. T. Harrison, *J. Chem. Soc., Chem. Commun.* **1972**, 231. [8b] I. T. Harrison, *J. Chem. Soc., Perkin Trans. 1* **1974**, 301. [8c] G. Agam, D. Graiver, A. Zilkha, *J. Am. Chem. Soc.* **1976**, *98*, 5206. [8d] G. Agam, A. Zilkha, *J. Am. Chem. Soc.* **1976**, *98*, 5214. [8e] G. Schill, W. Beckmann, N. Schweickert, H. Fritz, *Chem. Ber.* **1986**, *119*, 2647. [8f] P. R. Ashton, M. Belohradský, D. Philp, J. F. Stoddart, *J. Chem. Soc., Chem. Commun.* **1993**, 1269. [8g] P. R. Ashton, M. Belohradský, D. Philp, N. Spencer, J. F. Stoddart, *J. Chem. Soc., Chem. Commun.* **1993**, 1274. [8h] D. H. Macartney, *J. Chem. Soc., Perkin*

Trans. 2 **1996**, 2775. [8i] M. Händel, M. Plevoets, S. Gestermann, F. Vögtle, *Angew. Chem.* **1997**, *109*, 1248; *Angew. Chem. Int. Ed. Engl.* **1997**, *36*, 1199.

[9] F. M. Raymo, K. N. Houk, J. F. Stoddart, *J. Am. Chem. Soc.* **1998**, *120*, 9318.

[10] [10a] G. Hübner, G. Nachtsheim, Q.-Y. Li, C. Seel, F. Vögtle, *Angew. Chem.* **2000**, *112*, 1315; *Angew. Chem. Int. Ed.* **2000**, *39*, 1269. Also, see: [10b] H. W. Gibson, S. Liu, P. Lecavalier, C. Wu, Y. X. Shen, *J. Am. Chem. Soc.* **1995**, *117*, 852. [10c] C. Heim, PhD Thesis, University of Bonn, **1998**. [10d]C. Heim, A. Affeld, M. Nieger, F. Vögtle, *Helv. Chim. Acta* **1999**, *82*, 746.

[11] A. Affeld, G. M. Hübner, C. Seel, C. A. Schalley, *Eur. J. Org. Chem.* **2001**, 2877.

[12] T. Felder, C. A. Schalley, *Angew. Chem.* **2003**, *115*, 2360; *Angew. Chem. Int. Ed.* **2003**, *42*, 2258.

[13] For earlier studies dealing with steric isotope effects, see: [13a] V. J. Shiner Jr., *J. Am. Chem. Soc.* **1956**, *78*, 2653. [13b] V. J. Shiner Jr., *J. Am. Chem. Soc.* **1960**, *82*, 2655. [13c] K. Mislow, R. E. O′Brien, H. Schaefer, *J. Am. Chem. Soc.* **1960**, *82*, 5512. [13d] L. Melander, R. E. Carter, *J. Am. Chem. Soc.* **1964**, *86*, 295. [13e] L. Melander, R. E. Carter, *Acta Chem. Scand.* **1964**, *18*, 1138. [13f] K. Mislow, R. Graewe, A. J. Gordon, G. H. Wahl Jr., *J. Am. Chem. Soc.* **1964**, *86*, 1733. [13g] C. Heitner, K. T. Leffek, *Can. J. Chem.* **1966**, *44*, 2567. [13h] H. C. Brown, G. J. McDonald, *J. Am. Chem. Soc.* **1966**, *88*, 2514. [13i] H. C. Brown, M. E. Azzaro, J. G. Koelling, G. J. McDonald, *J. Am. Chem. Soc.* **1966**, *88*, 2520. [13j] G. J. Karabatsos, G. C. Sonnichsen, C. G. Papaioannou, S. E. Scheppele, R. L. Shone, *J. Am. Chem. Soc.* **1967**, *89*, 463. [13k] A. J. Kresge, R. J. Preto, *J. Am. Chem. Soc.* **1967**, *89*, 5510. [13l] R. E. Carter, L. Dahlgren, *Acta Chem. Scand.* **1969**, *23*, 504. [13m] R. E. Carter, L. Dahlgren, *Acta Chem. Scand.* **1970**, *24*, 633. [13n] R. E. Carter, L. Melander, *Adv. Phys. Org. Chem.* **1973**, *10*, 1. [13o] S. A. Sherrod, R. L. da Costa, R. A. Barnes, V. Boekelheide, *J. Am. Chem. Soc.* **1974**, *96*, 1565. For a review on isotope effects on non-covalent interactions, see: [13p] D. Wade, *Chem.-Biol. Interact.* **1999**, *117*, 191.

[14] [14a] G. M. Hübner, J. Gläser, C. Seel, F. Vögtle, *Angew. Chem.* **1999**, *111*, 395; *Angew. Chem. Int. Ed.* **1999**, *38*, 383. [14b] C. Reuter, W. Wienand, G. M. Hübner, C. Seel, F. Vögtle, *Chem. Eur. J.* **1999**, *5*, 2692. [14c] C. Reuter, F. Vögtle, *Org. Lett.* **2000**, *2*, 593. [14d] C. Seel, F. Vögtle, *Chem. Eur. J.* **2000**, *6*, 21. [14e] C. A. Schalley, G. Silva, C. F. Nising, P. Linnartz, *Helv. Chim. Acta* **2002**, *85*, 1578. [14f] X.-y. Li, J. Illigen, M. Nieger, S. Michel, C. A. Schalley, *Chem. Eur. J.* **2003**, *9*, 1332. Also, see: [14g] P. Ghosh, O. Mermagen, C. A. Schalley, *Chem. Commun.* **2002**, 2628. [14h] J. A. Wisner, P. D. Beer, N. G. Berry, B. Tomapatanaget, *Proc. Natl. Acad. Sci. (USA)* **2002**, *99*, 4983. [14i] J. A. Wisner, P. D. Beer, M. G. B. Drew, M: R. Sambrook, *J. Am. Chem. Soc.* **2002**, *124*, 12469.

[15] It should be noted that the Arrhenius and the Eyring activation parameters basically give the same results. Although E_A is not identical with $\Delta H^{\ddagger}$, they are both closely connected to each other via $E_A = \Delta H^{\ddagger} + RT_m$ (T_m is the average temperature of the temperature range of the experiment). Similar arguments apply to the pre-exponential factor of the Arrhenius equation and the activation entropy: $A = (ekT_m/h \exp(\Delta S^{\ddagger}/R)$. Consequently, E_A contains the enthalpic contributions, while A is a measure for the entropic effects. See: H. M. Frey, R. Walsh, *Chem. Rev.* **1969**, *69*, 103.

[16] [16a] S. J. Weiner, P. A. Kollman, D. A. Case, U. C. Singh, G. Alagona, S. Profeta, P. Weiner, *J. Am. Chem. Soc.* **1984**, *106*, 765. [16b] S. J. Weiner, P. A. Kollman, N. T. Nguyen, D. A. Case, *J. Comput. Chem.* **1987**, *7*, 230. [16c] D. M. Ferguson, P. A. Kollman, *J. Comput. Chem.* **1991**, *12*, 620.

[17] Schrödinger, Inc. 1500 SW First Avenue, Suite 1180, Portland, OR 97201, USA. Also, see: [17a] F. Mohamadi, N. G. Richards, W. C. Guida, R. Liskamp, C. Caulfield, G. Chang, T. Hendrickson, W. C. Still, *J. Comput. Chem.* **1990**, *11*, 440. [17b] D. Q. McDonald, W. C. Still, *Tetrahedron Lett.* **1992**, *33*, 7743.

[18] CACHE 5.0 for Windows, Fujitsu Ltd. **2001**, Krakow, Poland.

[19] For more sophisticated theoretical approaches to the problem of molecular motion in mechanically bound molecules, see: [19a] M. S. Deleuze, D. A. Leigh, F. Zerbetto, *J. Am. Chem. Soc.* **1999**, *121*, 2364. [19b] D. A. Leigh, A. Troisi, F. Zerbetto, *Angew. Chem.* **2000**, *112*, 358; *Angew. Chem. Int. Ed.* **2000**, *39*, 350.

[20] [20a] P. D. Boyer, *Angew. Chem.* **1998**, *110*, 2424; *Angew. Chem. Int. Ed.* **1998**, *37*, 2296. [20b] J. E. Walker, *Angew. Chem.* **1998**, *110*, 2438; *Angew. Chem. Int. Ed.* **1998**, *37*, 2308.

[21] C. A. Schalley, A. Lützen, M. Albrecht, *Chem. Eur. J.*, in press.

[22] For some selected reviews on molecular machines, see: [22a] K. E. Drexler, *Annu. Rev. Biophys. Biomol. Struct.* **1994**, *23*, 377. [22b] V. Balzani, M. Gómez-López, J. F. Stoddart, *Acc. Chem. Res.* **1998**, *31*, 405. [22c] J.-P. Sauvage, *Acc. Chem. Res.* **1998**, *31*, 611. [22d] J.-P. Collin, P. Gaviña, V. Heitz, J.-P. Sauvage, *Eur. J. Inorg. Chem.* **1998**, 1. [22e] Z. Asfari, J. Vicens, *J. Incl. Phenom. Macrocyc. Chem.* **2000**, *36*, 103. [22f] V. Balzani, A. Credi, F. M. Raymo, J. F. Stoddart, *Angew. Chem.* **2000**, *112*, 3484; *Angew. Chem. Int. Ed. Engl. Ed.* **2000**, *39*, 3348. [22g] C. A. Schalley, K. Beizai, F. Vögtle, *Acc. Chem. Res.* **2001**, *34*, 465. [22h] J.-P. Collin, C. Dietrich-Buchecker, P. Gaviña, M. C. Jimenez-Molero, J.-P. Sauvage, *Acc. Chem. Res.* **2001**, *34*, 477. [22i] A. W. Shipway, I. Willner, *Acc. Chem. Res.* **2001**, *34*, 421. [22j] A. R. Pease, J. O. Jeppesen, J. F. Stoddart, Y. Luo, C. P. Collier, J. R. Heath, *Acc. Chem. Res.* **2001**, *34*, 433. [22k] R. Ballardini, V. Balzani, A. Credi, M. T. Gandolfi, M. Venturi, *Acc. Chem. Res.* **2001**, *34*, 445. [22l] A. Harada, *Acc. Chem. Res.* **2001**, *34*, 445. [22m] C. A. Schalley, *Angew. Chem.* **2002**, *114*, 1583; *Angew. Chem. Int. Ed.* **2002**, *41*, 1513. [22n] T. Felder, C. A. Schalley, *Artificial Rotary Motors Based on Rotaxanes* in: *Bio-organic Chemistry II* (Eds.: H. Wennemers, C. Schmuck), Wiley-VCH, Weinheim, in press.

[23] [23a] C. A. Hunter, *J. Chem. Soc., Chem. Commun.* **1991**, 749. [23b] C. A. Hunter, *J. Am. Chem. Soc.* **1992**, *114*, 5303. [23c] F. Vögtle, S. Meier, R. Hoss, *Angew. Chem.* **1992**, *104*, 1628; *Angew. Chem. Int. Ed. Engl.* **1992**, *31*, 1619. Also, see: [23d] S. Ottens-Hildebrandt, T. Schmidt, J. Harren, F. Vögtle, *Liebigs Ann.* **1995**, 1855. [23e] R. Jäger, M. Händel, K. Rissanen, F. Vögtle, *Liebigs Ann.* **1996**, 1201. [23f] F. Vögtle, R. Jäger, M. Händel, S. Ottens-Hildebrandt, W. Schmidt, *Synthesis* **1996**, 353.

Received July 25, 2003

